Revealing the Potential of Waste Fibers from Timber Production and Clearings for the Development of Local Bio-based Insulation Fiberboards in French Guiana

Julie Bossu, Jérome Moreau, Christine Delisée, Nicolas Le Moigne, Stéphane Corn, Rodolphe Sonnier, Amandine Viretto, Jacques Beauchene, Bruno Clair

Revealing the potential of Guianese waste fibers from timber production and clearings for the development of local and bio-based insulation fiberboards.

Julie Bossu (julie.bossu@cnrs.fr)
ECOFOG: Ecologie des forets de Guyane https://orcid.org/0000-0001-6603-739X
Jérome Moreau
École supérieure du bois: Ecole superieure du bois
Christine Delisée
Université de Bordeaux: Universite de Bordeaux
Nicolas Le Moigne
IMT Mines Alès: Institut Mines-Telecom Mines Ales
Stéphane Corn
IMT Mines Alès: Institut Mines-Telecom Mines Ales
Rodolphe Sonnier
IMT Mines Alès: Institut Mines-Telecom Mines Ales
Amandine Viretto
CIRAD Montpellier-Occitanie
Jacques Beauchene
ECOFOG: Ecologie des forets de Guyane
Bruno Clair
LMGC: Laboratoire de Mecanique et Genie Civil

Research Article

Keywords: Tropical biomass valorization, residual fibers, bio-circular economy, insulation fiberboards, microstructure, thermal properties.

Posted Date: August 31st, 2022

DOI: https://doi.org/10.21203/rs.3.rs-1942491/v1

Title page

Title

Revealing the potential of Guianese waste fibers from timber production and clearings for the development of local and bio-based insulation fiberboards.

Author information

Julie Bossu[1*], Jérôme Moreau[2,3], Christine Delisée[3], Nicolas Le Moigne[6], Stéphane Corn[7], Rodolphe Sonnier[6], Amandine Viretto[5], Jacques Beauchêne[4], Bruno Clair[8]

[1] EcoFoF, CNRS, Kourou, Guyane
[2] Limbha, Ecole Supérieure du Bois, Nantes
[3] Département GCE, I2M, Bordeaux
[4] Ecofog, CIRAD, Guadeloupe
[5] BioWooEB, Univ. Montpellier, CIRAD, Montpellier, France
[6] Polymers Composites and Hybrids (PCH), IMT Mines Ales, Ales, France
[7] LMGC, IMT Mines Ales, Univ Montpellier, CNRS, Alès, France
[8] LMGC, Montpellier, France
***julie.bossu@cnrs.fr**

Abstract

In French Guiana, the development of bio-circular value chains to convert residual biomass into insulation fiberboard represents a promising opportunity to build energy-efficient houses. The objectives of this work are to select and characterize resources of interest and discuss the relationships between fiber properties, manufacturing parameters and fiberboards performances. Five local wood and bark residuals fibers are fractionated and fractions are analyzed by laser granulometry, thermal gravimetric analysis (TGA) and pyrolysis combustion flow calorimeter (PCFC). Fiberboards are produced using a thermomechanical process and their microstructure, thermal and sorption properties are characterized by X-ray microtomography, hot plate technique, and dynamic vapor sorption (DVS). Morphological analysis shows that large and elongated wood fractions allow the formation of thick and cohesive fibrous networks, while the bark small-sized fractions are more difficult to process, requiring more compaction and synthetic fibers as additives. However, despite processing difficulties, bark fiberboards show the best insulation performances, comparable to commercial reference products. In addition, TGA and PCFC tests reveal that bark fibers show better thermal stability and fire behavior compared to wood. Finally, they also show a strong affinity for water, highlighting the need for further investigations on their ageing under tropical conditions of use.

Keywords

Tropical biomass valorization, residual fibers, bio-circular economy, insulation fiberboards, microstructure, thermal properties.

Graphical abstract

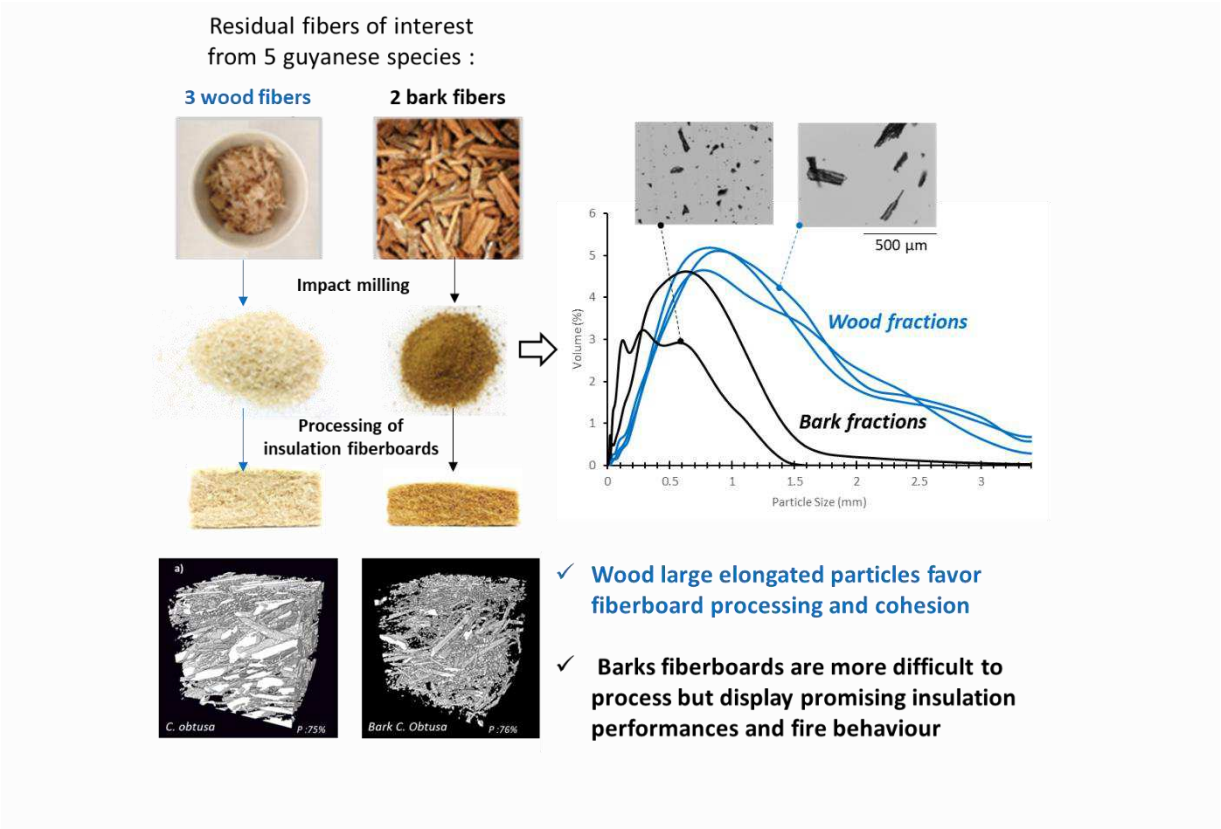

Statement of Novelty

This work constitutes the first attempt to explore the potential of Guyanese residuals biomass to produce insulation fiberboards, in alignment with the objective of developing sustainable constructive solutions adapted to tropical regions. The interdisciplinary experimental strategy developed here is innovant and enables discussing the relations between fibers morphology, fiberboards' microstructure and their final use performances. The outcomes of this work will help driving the selection of new resources to be considered for fiberboard production in French Guiana, and help identifying the key processing parameters to be controlled. Our results highlight two promising residual fibers for fiberboard production, evidencing similar to better insulation properties than the ones reported for commercial reference products. This work paves the way towards future research projects.

Text

INTRODUCTION

French Guiana is located in the Amazon region, a hot and humid area. To provide comfortable living conditions, the methods and materials used for buildings construction must guaranty good solar protection and regulation of humidity. In the past, local traditional houses were designed using passive architecture methods and durable massive wood elements. Today, because of the extreme demographic growth observed in the region (around 120 000 houses would need to be built by 2040, according to the regional environment, planning and housing agencies, DEAL, 2018), the building of traditional houses has been progressively replaced by large-scale construction of less expensive and poorly ventilated western-styled houses. The massive use of air-conditioning used to refresh and dry interior parts represents a large share of domestic energy consumption. To support ecological transition, efficient and affordable biomaterials must be developed to improve houses' energy efficiency and encourage the next generation to change the path towards sustainable housing. Today, most of the insulating products used in French Guiana are imported with high transportation costs, based on fossil sources and non-adapted to high-moisture conditions. A long-term objective of the region is to shift toward local production of bio-based materials for sustainable construction. To do so, the use of wood fibers can be considered as a promising perspective to produce high-performance insulating materials [1]. Indeed, natural fibers exhibit several benefits compared to conventional mineral and synthetic fibers: low density, good specific mechanical properties, non-abrasive properties, low acoustic and thermal conductivity and biodegradability, and ability to maintain hygrothermally stable room conditions thanks to their high hydric inertia [2, 3].

Regarding the manufacturing of insulation fiberboards, the non-woven process appears to be a promising technological solution: this technique, adapted from the textile industry, uses a thermo-mechanical process where the cohesion of the fiber mat is mostly ensured by the interlocking of the fibers [4]. It requires light industrial equipment, as well as a small proportion of synthetic fibers, and could be easily developed in French Guiana. With regard to the fiber resources available among the local biodiversity, the preferred option is to consider using residual biomass, in order to avoid further exploration of the Amazonian rainforest. Waste wood fibers resulting from timber production operations are available, abundant and qualitative (species selected and explored for their good technical performances). Two Guyanese commercial species were selected: *Dicorynia guianensis* and *Sextonia rubra*, representing 62.4 % of the local timber production (data from the National Forest Office, 2020). In parallel, small-sized trees of fast-growing species are frequently cut during clearings but remain non-valorized. Again, two species have been selected: *Cecropia obtusa,* the most abundant in French Guiana, also harvested for the extraction of the high-value chemical compounds found in its bark; and *Virola surinamensis*, which has also been proved to produce a large amount of bark showing well defined fiber bundles [5], expected to be easily isolated during defibering operations.

The general objective of this study was to assess the potential of these Guyanese residual fibers for the production of insulation fiberboards adapted to tropical environment, since the development of such materials still faces important knowledge gaps:

- *The quality of the tropical species studied here has never been evaluated at fiber scale.*

First, it is difficult to anticipate the achievable quality of the milled fractions. The selected wood and bark specimens are characterized by different anatomical microstructure (cells type, shape and organization), densities and chemical composition, which are expected to influence the final particles size distribution and morphology of the fractions after milling. Moreover, we have no information about the thermal properties and reaction to fire of these materials, which is of prior interest when it comes to insulating materials intended to be used for building and construction.

- *The manufacturing process of fiberboards has never been adapted to tropical resources*.

Previous works have been conducted with wood fibers from pine, poplar and eucalyptus of 2 mm length [6], but tropical wood and bark fibers characterized by different structures and morphology have never been tested. The process parameters need to be optimized, since the specificities of tropical resources might influence their conversion into fiberboards.

- *The relations between fiber characteristics and fiberboard properties are understudied.*

Since no glue was used during the production of fiberboards, thermal conductivity is expected to depend on the intrinsic properties of the fibers, as well as the resulting microstructure and porosity distribution within the fiber mat [7]. This raises the question of which is the most important parameter to be taken into account when selecting quality fibers for the production of insulation fiberboards: What is the effect of fiber morphological features on microstructure and porosity of fiberboards? Does the microstructure dominate over the intrinsic insulating properties of the fibers?

The specific goals of the present study were therefore to (i) characterize the morphological and thermal properties of the selected tropical waste fibers and particles obtained after milling; (ii) optimize the production process for each resource; (iii) discuss the microstructure-properties relationships; (iv) report on the final achievable insulation performance and water affinity of the produced fiberboards, and (v) propose solutions for process improvement.

This work constitutes, to our knowledge, the first attempt to study the thermal properties of Guyanese waste fibers and their suitability for the production of insulation fiberboards.

MATERIAL AND METHODS

Selection of resources

For commercial wood species *Dicorynia guianensis* Amsh. (*D. guianensis*) and *Sextonia rubra* (Mez) van der Werff (*S. rubra*), a residual heartwood board resulting from sawing operations in the laboratory was selected. For fast-growing species, wood and barks fibers from *Cecropia obtusa* Trécul (*C. obtusa;* Bark *C. obtusa*) and bark fibers from *Virola surinamensis (Rol. ex Rottb.) Warb.* (Bark *V. surinamensis*) were collected on young specimens (5 m height, approximately 2 years-old) harvested in a secondary forest near the Paracou experimental station (5°16'27N; 52°55'26W).

Our final sampling thus consisted in 3 wood samples and 2 bark samples that appeared to be promising resources to be considered for the development of a local sustainable value chain to produce insulation fiberboards (Figure 1). The main characteristics of each wood species, based on past surveys on Guyanese wood properties

(Gérard et al. 2016; Gérard et al. 2019) are given in Table 1. No information could be found in the literature for the studied barks.

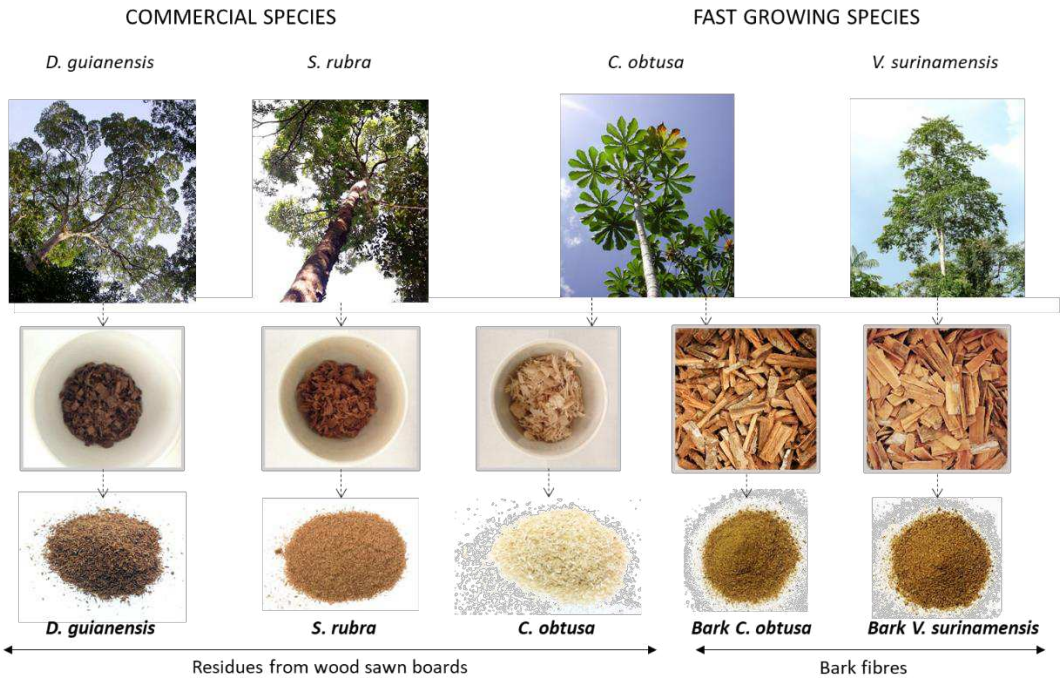

Figure 1. Sampling strategy. Wood fibers were collected from *D. guianensis, S. rubra* and *C. obtusa*. Bark fibers were collected from *C. obtusa* and *V. surinamensis*. Fibers were oven-dried at 60°C for 3 days and milled into fine powder using an impact mil SM 300 (1.5 kg/h and 2000 rpm with 4 mm then 2 mm grid). Photos credits: *D. guianensis* : Romain Lehnebach ; *S. rubra*: Emeline Houël; *C. obtusa*: Yves Caraglio; *V. surinamensis*: Inventaire National du Patrimoine Naturel.

Table 1. Wood physical and chemical characteristics based on past surveys on Guyanese wood properties (Gérard et al. 2016; Gérard et al. 2019). N: number of tested specimens; D12: wood density at 12% of relative humidity; FSP: Fiber Saturation Point. Standard deviation is given in brackets. Cellulose and lignin contents were measured by the Kürschner and Klason methods respectively. Extractives were extracted in water. *Database reports measurement performed on *Cecropia* genus without specifying the studied species.

	Physical properties			Biochemical composition				
SPECIES	N	D12	FSP (%)	N	Cellulose (%)	Lignin (%)	Extractives (%)	Ashes (%)
D. guianensis	90	0.79 *(0.05)*	28.6 *(2.3)*	7	45.5 *(2.0)*	35.9 *(2.1)*	4.4 *(1.5)*	0.7 *(0.3)*
S. rubra	28	0.66 *(0.04)*	29.4 *(2.8)*	3	47.8 *(2.7)*	31.7 *(3.3)*	9.1 *(2.7)*	0.4 *(0.2)*
*Cecropia sp**	6	0.32 *(0.06)*	40.7 *(3.7)*	2	52.5	23.3 *(1.2)*	4.8 *(1.5)*	1.2 *(0.3)*

Fibers' production and characterization

Fibers' production

In previous studies on softwood, fiberboards were successfully manufactured from fibers with an average length of 1.6 mm [8]. To achieve such dimensions, an impact mill has been used. This technology enables to reach a satisfying comminution of ligno-cellulosic materials while limiting energy consumption [9]. More than 2 kg of material were collected for each resource. Samples were manually cut into chips and air-dried in the laboratory during one month. Chips were first oven-dried at 60°C for 3 days to avoid caking during grinding. Thereafter,

chips were fractionated into fine powder (Figure 1) using an impact milling system (SM 300, Retsch) in continuous mode, at 1.5 kg/h and 2000 rpm; two fractionation steps were carried out, using 4 mm and 2 mm grids successively. A final dry mass of 1.3 kg per resource was produced.

Morphological analysis

The morphological analysis has been performed on the PLANET platform (UMR IATE, Montpellier). The particle size distributions of the studied fractions were analyzed with a laser granulometer (LS 13 320 XR, Beckman Coulter) in dry mode. Five replicates of 5 g per material were tested, showing good reproducibility.

Mean diameter (d50) and specific surface area (SSA) were determined for each sample. In addition, the milled fractions were automatically air-sprayed onto a glass slide and analyzed using a particles shape analyzer (Morphologi 4, Malvern). High-definition images of each isolated particle were recorded, providing reliable and accurate data for the determination of particles' shape parameters (circularity and elongation). A mean number of 47 727 particles were analyzed for each sample.

Thermal Gravimetric Analysis (TGA)

TG experiments have been carried out to study the thermal behavior of the milled fibers during pyrolysis under oxygen atmosphere, using a Mettler TGA2 apparatus (Schwerzebbach, Switzerland) equipped with a XP5U balance. About 10 mg of each sample was heated from room temperature to 500 °C under air flow (50 mL.min^{-1}) at a heating rate of 10 °C.min^{-1}. Onset temperature (T_{onset}) was computed as the intersection point of the extrapolated baseline and the inflectional tangent at the beginning of the degradation peak. The peak degradation temperatures (T_{peak}) were taken at the maximum values of the mass-loss derivative curve. Analysis was done in duplicate for each sample with good reproducibility.

Pyrolysis combustion flow calorimeter

Tests were carried out using a Fire Testing Technology microcalorimeter. 2 (±1) mg of sample was heated under nitrogen flow up to 750 °C at a heating rate of 1 °C/s. The released gases were mixed with oxygen (N_2/O_2 80/20) and burned into a combustion chamber at 900 °C. Under these conditions, the combustion is guaranteed to be complete. Heat release rate (HRR) was calculated from the oxygen consumption according to Huggett's relation [21] (1 kg of consumed oxygen corresponds to 13.1 MJ of heat release). Each test was performed twice. The quantity of char, the peak of heat release rate (pHRR) and corresponding temperature (T(pHRR)), the total heat release (THR), and the heat of complete combustion (ΔH, calculated as the ratio between THR and mass loss) were determined.

Fiberboard's processing and characterization

Non-woven fiberboards' processing

This first step was carried out using an air-laid machine from Laroche (Figure 2). Firstly, wood/bark fractions were carded with a rotating spiked roller (1100 to 2300 rpm), mixed with 6 mm-length synthetic bicomponent fibers

(polyester/polypropylene, adjustable quantity around 10% of addition per mass of natural fibers) and blown (at 0.5 to 2 $m.min^{-1}$) onto a vacuum perforated drum. Fibers in air-laid webs tended to be isotropically oriented in horizontal plane. Mat consistency was modulated by the stretching ratio (speed of entry delivery roller / speed of exit pressure rollers; adjustable from 0.5 to 2). Machine settings were adjusted in order to obtain a homogeneous fiber mat in mass and thickness. The formed fiber mats were then superimposed to form a fiberboard. At this stage, the cohesion of the fiberboard was only ensured by the entanglement of fibers.

Figure 2. Processing equipment used for 3D fiberboard formation: napper opener machine from Laroche.

Non-woven fiberboard consolidation

This second processing step was carried out using a hot-air oven from Strahm (Figure 3). This is a dry bonding process that takes advantage of the thermoplastic properties of synthetic fibers. This thermal post-treatment results in very low density non-woven fibrous structures with good cohesion. The operating temperature for melting the thermoplastic fiber sheath has been set at 160°C.

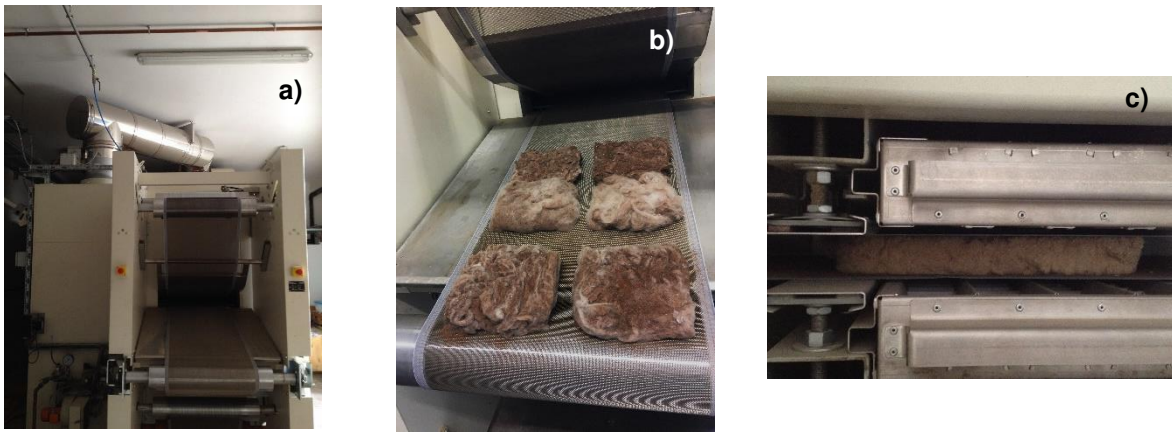

Figure 3. Processing equipment used for insulation fiberboard consolidation: a) hot air oven from Strahm b) fiberboard at the entrance of the oven c) fiberboard in the cooling part of the oven.

Fiberboards' characterization

- *3D microstructure*

The internal microstructure of the fiberboards was characterized through a non-destructive imaging technique, using a SkyScan X-ray microtomograph. First, a small cylindrical sample of 9-mm diameter and 10-mm height is

carefully extracted from the initial fiberboards. The X-ray beam passes through the sample and the signal transmitted is recorded by CCD sensors. After 3D reconstruction of X-ray projections, a subvolume is extracted from the grey level 3D images to remove borders and to avoid any boundary effect, induced both by the cutting of the sample and the X-Ray conic source. The size of the pores of a set of wood/bark fibers was measured by performing successive openings of growing size on the virtual volume. The 3D images resolution was 6.9 microns/voxel and the analyzed volume was 5.5 x 5.5 x 5.5 mm^3.

- *Insulation properties*

Insulation properties of the fiberboards were measured on 100 x 100 x *e* mm^3 samples (with *e* the thickness of the fiberboard, samples stabilized at 20 °C and 65 % of relative humidity.) by the hot plate technique, with a Desprotherm device (Epsilon Alcen). The thermal imbalance of the sample was induced by providing a uniform and unidirectional heat flow on one of its isolated faces. The apparent thermal conductivity λ^*_{app} ($W.m^{-1}.K^{-1}$) of the material could be calculated by assessing its equivalent thermal effusivity *b* ($W.K^{-1}.m^{-2}.s^{1/2}$) and its bulk volumetric heat capacity $\rho^*.C_p$ ($W{\cdot}m^{-3}{\cdot}K^{-1}$), where ρ^* *(kg* m^{-3}*)* is the bulk density and C_p ($W\ kg^{-1}{\cdot}K^{-1}$) is the specific heat capacity *(Equation 1)*. Measurements were done in triplicate.

$$\lambda^*_{app} = \frac{b^2}{\rho^* \cdot C_p} \qquad \textit{(Equation 1)}$$

- *Dynamic Vapor Sorption (DVS)*

Sorption measurements were performed by dynamic vapor sorption (DVS), using a gravimetric sorption instrument (Service Solution Limited, UK, London). Each fiberboard specimen (10 +/-2mg) was air-dried during two weeks prior loading in the instrument at RH = 0%. Mass changes were constantly recorded along five different relative humidity stages (RH = 0%, 25%, 50%, 75% and 90%). Stabilized mass was recorded after reaching a mass variation ratio dm/dt below 0.001 $\%.min^{-1}$, allowing the calculation of the moisture content (MC). These conditions have been shown to be adequate for reaching constant mass uptake at each step of water vapor sorption for wood and biomaterials [10, 11]. The specific mass stabilization time ($SMST_{75>90\%RH}$), was calculated as the time per mass unit necessary to reach equilibrium after a change in RH from 75% to 90% (Equation 2).

$$SMST_{75>90\%RH} = \frac{mass\ stabilization\ time\ from\ RH{=}75\%\ to\ 90\%}{Stabilized\ mass_{RH=0\%}} \qquad \textit{(Equation 2)}$$

RESULTS AND DISCUSSION

Morphological and thermal properties of wood and bark fractions

- *Morphological analysis*

Considering all specimens, morphological characterization of the milled fractions by laser granulometry revealed that most of the ground particles were much smaller than 2 mm (average d_{50} of 0.56 mm for all tested fractions)

(Figure 4). Indeed, many authors have already reported particle sizes much smaller than the grid opening after impact milling operations. Using a 2 mm grid and a similar milling protocol to the one used in this study, Mayer-Laigle et al. (2018), David (2019) and Rajaonarivony et al. (2019) all observed average particle sizes below 0.7 mm, using wheat straw, vine shoots and pine barks fibers, respectively. It thus appears reasonable in our case, studying short-length tropical hardwood fibers, to obtain such dimensions.

At the inter-specific level, it can be noticed that identical milling conditions resulted in fractions of variable size distributions depending on the species (Figure 4 and Table 2). All wood specimens showed similar size distributions (d_{50} = 0.73 mm +/-0.051 mm), whereas milling bark specimens resulted in smaller particles (d_{50} = 0.42 and 0.21 mm for *Bark V. surinamensis* and *Bark C. obtusa*, respectively). Since no subsequent sieving operation was conducted after milling, a large amount of fine particles has thus been obtained for bark specimens as illustrated in Figure 4. Maharani et al. (2010) studied the effect of different mill types on five different tropical species. They showed that impact milling leads to the highest content of fine particles under 0.3 mm (around 71.8%, in volume). We used a similar classification to sort the different fractions produced in this study (oversized particles > 0.7 mm; 0.7 mm < coarse particles < 0.3 mm; fines particles < 0.3 mm). The results obtained showed that there is a large amount of coarse and fine particles in all fractions (minimum 50 % in volume), and confirmed the existence of maximal amounts of fine particles for the bark specimens (up to 66.8 % in volume for *Bark C. obtusa* and 40.3 % in volume for *Bark V. surinamensis*) (Figure 5). Most likely, the small dimensions obtained for both bark specimens indicate their lower resistance to impact milling and their tendency to break into shorter length fractions compared to wood fibers.

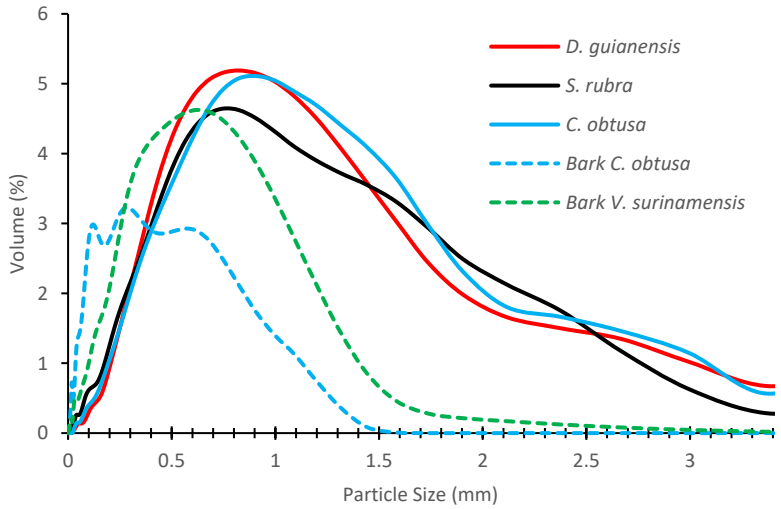

Figure 4. Particle size distribution of the milled fractions for each tested material measured by laser granulometry (LS 13 320 XR, Beckman Coulter).

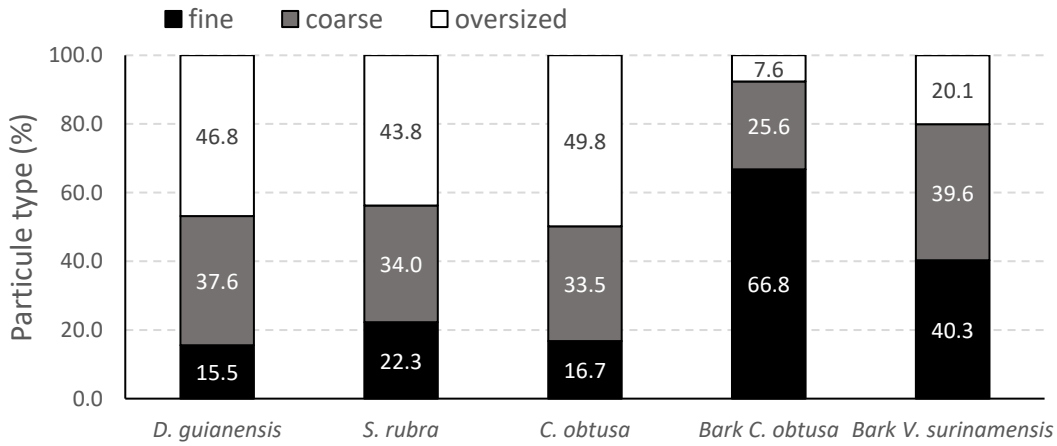

Figure 5. Representation of the particle size distribution of wood and bark powder samples over three dimensional categories: oversized (OS) > 700 µm; coarse particle size (CPS) : [300-700 µm]; fine particle size (FPS) : [100-300 µm].

Optical observations of air-sprayed fractions confirmed the size distributions previously obtained, showing larger and lengthen particles for wood samples compared to bark samples (Figure 6). In addition, this method allows a better characterization of the particle aspect ratio, revealing that *S. rubra* and *C. obtusa* wood fractions were composed of a larger share of elongated elements, while *D. guianensis,* and bark fibers even more extensively, displayed smaller and circular elements (Table 2).

The fractions produced in this study are therefore quite dissimilar in terms of morphology, but representative of the achievable quality that can be obtained using raw residual biomass from the wood industry sector, which is the focus of this study. However, the milling process could be optimized if willing to attain a specific particle size. For example, the initial drying step could be reduced since it has been shown to negatively impact fibers' mechanical properties and load-bearing capacities during milling by limiting the plasticizing effect of water, resulting in the generation of a larger share of fine particles [9]. Also, the rotation speed and the milling time could be reduced to limit the degradation of the fibers. Thereafter, subsequent sieving operations could be applied to select a specific particle size class while maintaining satisfactory milling yields. It would also be possible to use another fiber separation method such as defibering, but such methods require heavy technical installations which might be difficult to implement in French Guiana for the foreseeable future.

The heterogeneous morphological characteristics of the fractions described in this section are expected to influence both the processing and the performances of the fiberboards. Specifically, while reduced fibers' length may complicate fiberboards shaping, it has been found that fine particles promote desirable microstructuration of the fiberboards and thus lead to interesting thermal properties (Vignon, 2020).

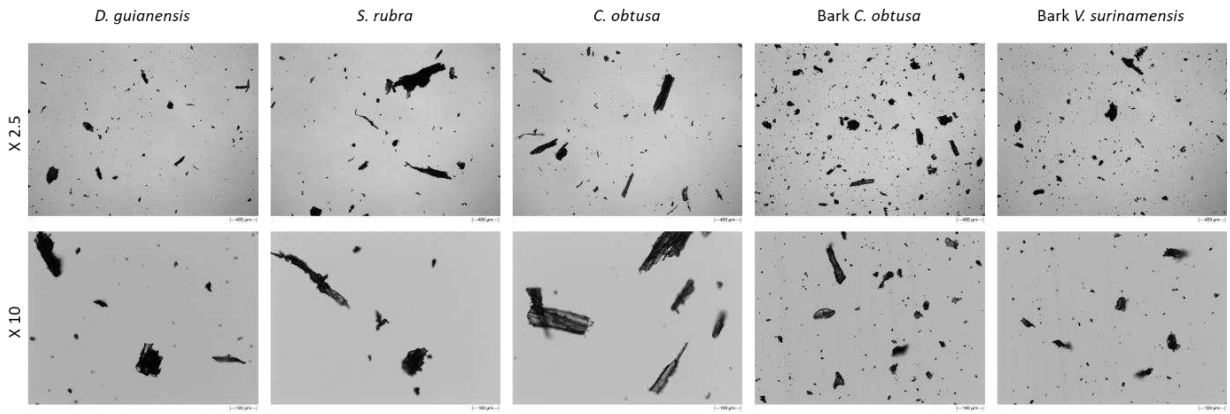

Figure 6 – Optical observations of the milled fibers air-sprayed on a glass plate using a particles shape analyzer (Morphologi 4, Malvern).

Table 2. Results of the morphological analysis of wood and bark fractions. N: number of detected elements; d_{50}: mean diameter; Elongation; Circularity; CV%: coefficient of variation.

Material	N	d_{50} (mm)	Elongation	Circularity	CV%
D. guianensis	67235	0.70	0.62	0.92	10.8
S. rubra	219852	0.69	0.72	0.86	3.4
C. obtusa	183148	0.79	0.70	0.89	6.7
Bark *C. obtusa*	320135	0.21	0.53	0.91	4.9
Bark *V. surinamensis*	118443	0.42	0.53	0.93	3.4

- *Thermal analysis*

Fiber samples were analyzed by thermal gravimetric analysis (TGA) to study their thermal decomposition kinetics (from room temperature up to 600°C at 10 °C.min^{-1}, under oxygen gas flow), and by Pyrolysis Combustion Flow Calorimeter (PCFC) (anaerobic pyrolysis and complete combustion) to characterize their flammability. Results are presented in Figure 7 and 8 and the characteristic values are reported in Table 3.

In this work, the thermal degradation was studied under aerobic pyrolysis conditions. Compared to anaerobic pyrolysis, far fewer studies have been published on biomass combustion. Indeed, thermal degradation under oxidative atmosphere is more complex, considering that the presence of an oxidizing agent (air, oxygen, etc.) generates reactions between oxygen and solid reactants [16–18]. All fractions started losing weight at about 200 °C (*i.e.*, 40 °C above the temperature used for fiberboards processing) and their degradation behavior was a complex process, composed of two apparent degradation stages: the first rapid weight loss corresponding to pyrolysis or devolatilization stage (Stage I. on Figure 7); then secondary weight loss corresponding to char oxidation due to the presence of oxygen (Stage II. on Figure 7) [19]. Under nitrogen flow, hemicelluloses and cellulose pyrolysis occurs around 295 °C and 370 °C, respectively [20]. The decomposition of lignin is slower and more complex since lignin fractions have different stabilities. This component thus covers a wider range of temperature from 200 °C to 450 °C under nitrogen [21]. In presence of oxygen, the devolatilization peaks appear at lower temperature (-15 °C and -35 °C for hemicelluloses and cellulose, respectively) [22]. As a result, specific degradation peaks of hemicelluloses and cellulose are expected around 280 °C and 340 °C in aerobic conditions (peaks (a) and (b) on Figure 7).

These values match the double peaks observed during pyrolysis of wood fractions *D. guianensis* and *S. rubra*. Both species showed similar behavior with almost identical cellulose degradation peaks (at 334 °C and 332 °C respectively, with identical intensity), likely because of their close chemical composition (Table 1). In contrast, pyrolysis of hemicelluloses and cellulose in *C. obtusa* wood fraction was more pronounced, and the cellulose degradation peak appeared at lower temperature (around 310 °C). This could possibly originates from its lower lignin content (around 23%, Table 1), which has been proved to decompose slowly during pyrolysis [23]. Char oxidation peak also occurred at lower temperature and was really marked, confirming its lower thermal stability compared to other samples. However, it has also been proved that the combination of a low content of lignin with a high content of cellulose, as it is the case for *C. obtusa*, could lead to charring and to incomplete combustion of these fibers, limiting their contribution to the heat evolved during burning.

Regarding bark samples, thermal stability is significantly higher compared to wood samples. Indeed, for the same species *C. obtusa*, degradation peaks were much less pronounced and shifted to higher temperatures for bark samples (around 320 °C), indicating that a higher activation energy is needed to decompose woody biomass, which could be the result of the presence of a higher amount and different type of lignin compared to wood [23]. *Bark V. surinamensis* showed the best thermal stability over the studied temperature range.

PCFC tests were also conducted to study the fire reaction of the studied fractions. Measured peak values (pHRR) are similar to the ones found in the literature for wood [24]. The heat release rates (HRR) versus temperature curves (Figure 8), confirmed that wood fibers have similar thermal behavior. The only difference between wood fibers concerned the temperature peak: T(pHRR) was observed to be lower for *C. obtusa*.

Bark samples released markedly less energy than woods, with pHRR equals to 71 W/g (compared to 147 W/g on average for wood fractions) and THR equal to approximatively 7 kJ/g (compared to 11.6 kJ/g on average for wood fractions). They also generate more char during their decomposition (750 °C): around 25% char (compared to 16.2% on average for wood fractions), which is desired since it enhances the fire resistance of materials: the material which forms carbonaceous char has a reduced ability to supply the gaseous fuels required to fuel the fire. ΔH represents the intrinsic energy of the release gases during combustion, and lower values were obtained for bark fractions. The higher quantity of chars formed from bark can explain this result, since chars store high quantities of carbon, which tend to reduce the energy of gases.

Bark fractions thus revealed better thermal stability and fire reaction compared to wood, which could originate from higher rates of extractives and/or lignin, which are associated with a high carbon content and result in higher yields of char [22]. Indeed the presence of specific chemical components such as suberin which contribute to shielding against heat-induced degradation [25] could also be responsible of the observed differences.

Table 3. Specific degradation temperatures determined from DTG thermograms.

	TGA measurements		Microcalorimeter measurements				
	$T_{50\%}$(°C)	T_{peak} (°C)	Char (%)	pHRR (W/g)	T(pHRR) (°C)	THR (kJ/g)	ΔH (kJ/g)
D. guianensis wood	347	334; 481	18.32	154	372	11.1	13.5

S. rubra	342	332; 465	15.55	146	363.5	12.7	15.0
C. obtusa	314	313; 406	14.79	141	341	11.1	13.0
Bark *C. obtusa*	352	325; 438	25.24	67.5	354.5	7.1	9.4
Bark *V. surinamensis*	395	315; 438	24.83	74	354	7	9.3

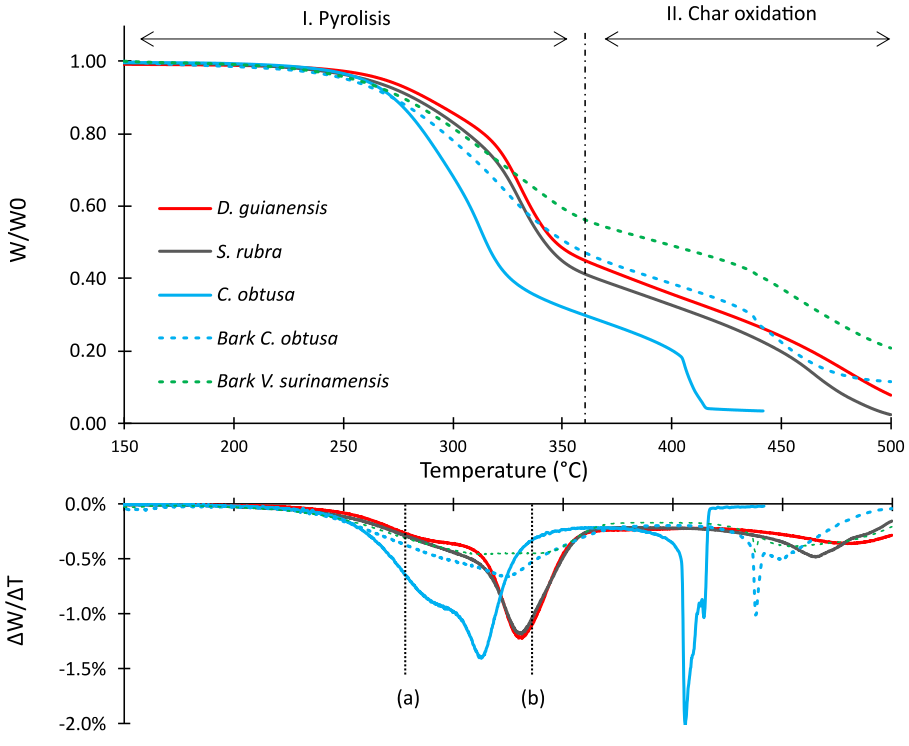

Figure 7. Results of the thermal analysis (TGA) performed on the studied fractions. Mass variations (top) and its derivative (bottom) during heating under air flux at 10°C.min^{-1} up to 500°C. Dotted lines (a) and (b) represent specific the specific degradation peaks of hemicelluloses and cellulose in oxidative conditions. Lignin degrades over a wider temperature range, from 350°C to 450°C.

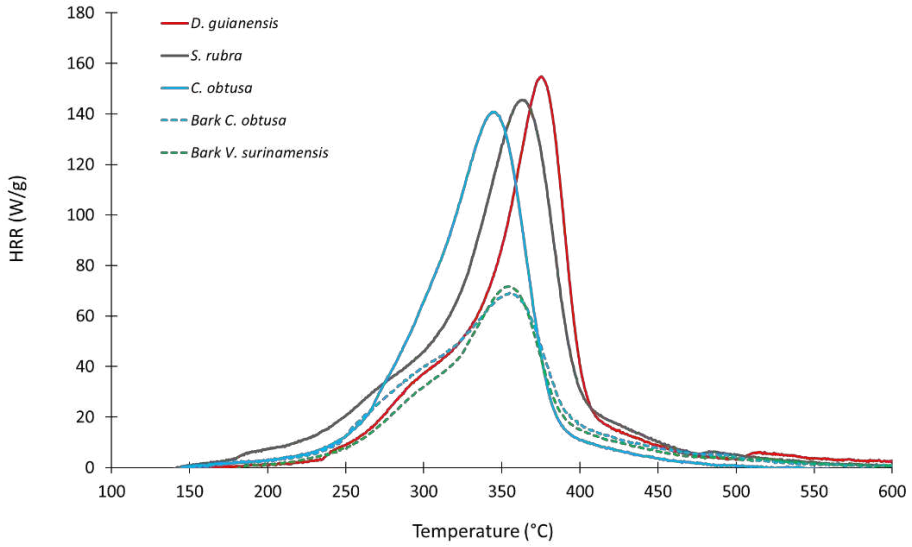

Figure 8. Results of the PCFC tests conducted on the studied fractions. The evolution of the heat release rates (HRR) is shown as a function of the pyrolysis temperature.

Fiberboard manufacturing and microstructure: effect of wood and bark fractions' morphology

Uniformity of air-laid webs depends on the degree of opening of the fibers, the proportion of synthetic fibers and the airflow profile. Processing parameters were first set based on previous works conducted with pine, poplar and eucalyptus fiber fractions of about 2 mm in length [6]. Using the same protocol with the small-sized fractions studied in this work, we first observed a severe mass loss during the web formation step (more than 80%) and a bad cohesion of the resulting fiber mats. Changes in the processing parameters have thus been operated. Firstly, to limit mass loss due to the aspiration of fine particles, air suction has been halved from 50 to 25%. Secondly, the initial opening step on the carding machine has been eliminated since no fiber tufts could be observed and because controlling fiber orientation was not possible for such small dimensions. On the contrary, opening step for synthetic fibers was enhanced (two successive opening steps were operated), to facilitate their mixing with lignocellulosic fibers and improve mat cohesion. Finally, the stretching ratio was decreased from 2 to 0.5 in order to increase the compaction of the mat and improve its cohesion. Thanks to these adjustments, average mass losses were greatly reduced (Table 4). However, the final results were still higher than the values reported by [15] for hardwood species (25% and 28% for poplar and eucalyptus respectively). It is clear that even after optimizing the process, the large share of fine particles present in the studied fractions remains an issue: the suction of the smallest particles leads to high mass losses.

As a result, a higher rate of synthetic fibers was needed to reach satisfying mat cohesion (from 8% for *C. obtusa* to 17% for Bark *C. obtusa*, compared to 6% for the reference pine fibers of 2 mm length, according to Vignon (2020)). Here, a strong negative correlation (Pearson's r = -0.99; p-value < 0.01) was found between fiber particle size (d_{50}) and the amount of synthetic fibers needed to reach satisfying cohesion (Figure 9a). As a result, the bark fibers-based fiberboards were composed of a higher proportion of synthetic fibers and more compact with thicknesses from 15 to 18 mm (Table 4 and Figure 10), which is expected to lower their insulation performances. *C. obtusa* and *S. rubra* fiberboards were the easiest to manufacture and resulted in the thickest mats (up to 30 mm) produced in this study (Table 4 and Figure 10). Comparing the morphological features of the fibers and the resulting thickness of the mats, we found a significant positive correlation (Pearson's r = 0.92; p-value < 0.01), with greater fibers elongation leading to greater mat thickness due to better cohesion (Figure 9b). Indeed, many researches have already reported that increasing fiber elongation is an efficient strategy to enhance the mechanical performances of paper and bio-composite materials. Fiber inter-bonding is favored, allowing the formation of a cohesive 3D interlocked fiber network [26, 27].

In summary, besides controlling the amount of fine particles, our results also showed that fiber elongation is a key morphological parameter to be considered to enhance the manufacturing and structuration of fiberboards. Besides morphological properties, the chemical composition of the fractions can also influence the microstructuration of the fiberboards during the heating phase and their adherence to synthetic fibers. Indeed, the chemical reactions and physical consolidation of the fibers induced by applied heat and pressure can favor self-bonding reactions in binderless fiberboards [28]. In particular, fibers with lignin-rich surfaces might fuse together as the softened lignin molecules flow from one fiber surface to another one, and possibly form covalent bonds [29]. In the case of the studied wood and bark fractions, a detailed analysis of their chemical composition will be necessary to better understand the mechanism at play.

Table 4. Processing parameters and key characteristics of the produced fiberboards from each wood/bark fraction. N: number of panels produced; Mass: average mass per panel sample; Loss rate: fractions' mass loss rate during mat forming processing steps; Synthetic fibers rate: amount of synthetic fibers added to the fractions to reach satisfying cohesion of the mat, optimized for each species; Thickness: final thickness of the mat after consolidation; Apparent density: bulk density of the mat at 20 °C, 65 % relative humidity. All fiberboards were consolidated at 160°C.

Material	N	Synthetic fibers Rate (%)	Mass (g)	Loss rate (%)	Thickness (mm)	Apparent density ($kg.m^{-3}$)
D. guianensis	4	10	401	53	22.0	203
S. rubra	4	10	500	38	25.5	267
C. obtusa	5	8	382	43	30.0	166
Bark C. obtusa	3	17	200	72	18.0	141
Bark V. surinamensis	3	15	293	66	15.2	202

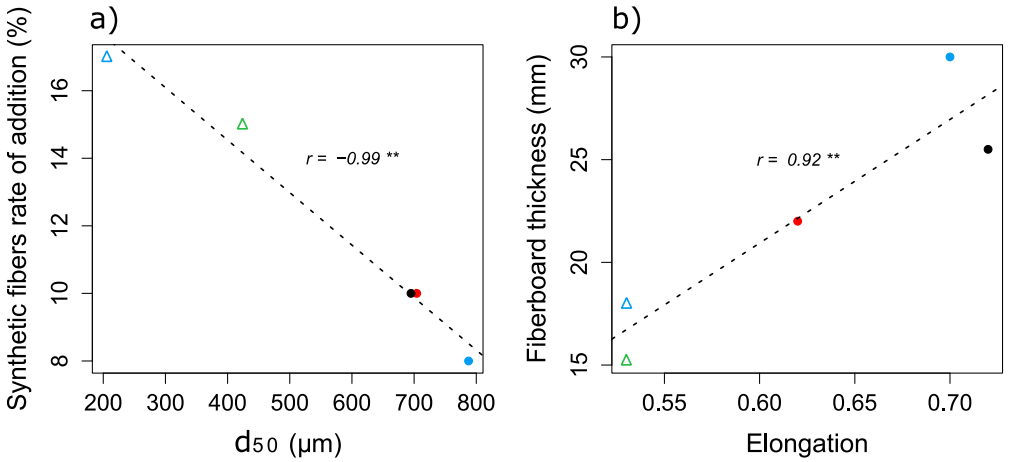

Figure 9. Influence of fiber size (a) and elongation (b) on the processing of fiberboards in terms of final thickness and synthetic fiber rate. Points stands for wood fiberboards (red: *D. guianensis*; black: *S. rubra*; blue: *C. obtusa*) and triangles for bark fiberboards (blue: Bark *C. obtusa*; green: Bark *V. surinamensis*); r : correlation coefficient of Pearson; **: p-value < 0.01.

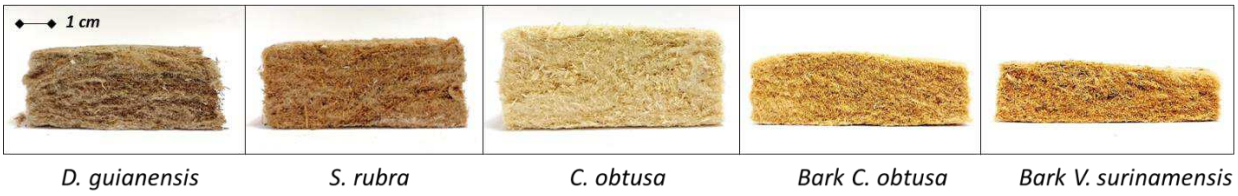

Figure 10. Final aspect of the produced insulation fiberboards from each wood/bark fraction.

The internal microstructure of the fiberboards produced from the two most contrasted fibers fractions in terms of morphological characteristics, i.e., *C. obtusa* (d_{50}: 0.79 mm; Elongation: 0.70) and Bark *C. obtusa* (d_{50}: 0.21 mm; Elongation: 0.53), was studied using X-ray microtomography. 3D volume elements were reconstructed from successive X-ray projections (Figure 11a). After cleaning and thresholding, successive openings by spheres of growing size were performed on the 3D images (Tran et al. 2013; Délisée et al., 2017; Hamdi et al. 2020). This

analysis enabled the determination of pore size distribution within the fiberboard thickness (Figure 11b). X-ray microtomography images confirmed that a larger share of large-sized and elongated particles can be observed in *C. obtusa* compared to Bark *C. obtusa*. As a result, these two fiberboards were characterized by different apparent densities (166 and 141 kg.m^{-3} for *C. obtusa* and Bark *C. obtusa* fiberboards respectively, Table 4). However, probably because of the large share of FPs observed in bark fractions, pore size distributions were similar for both fiberboards, with slightly larger pores observed for Bark *C. obtusa* (average distance between two fibers of 323 µm compared to 297 µm for wood; total porosity: 75% for wood and 76% for bark) (Figure 11b).

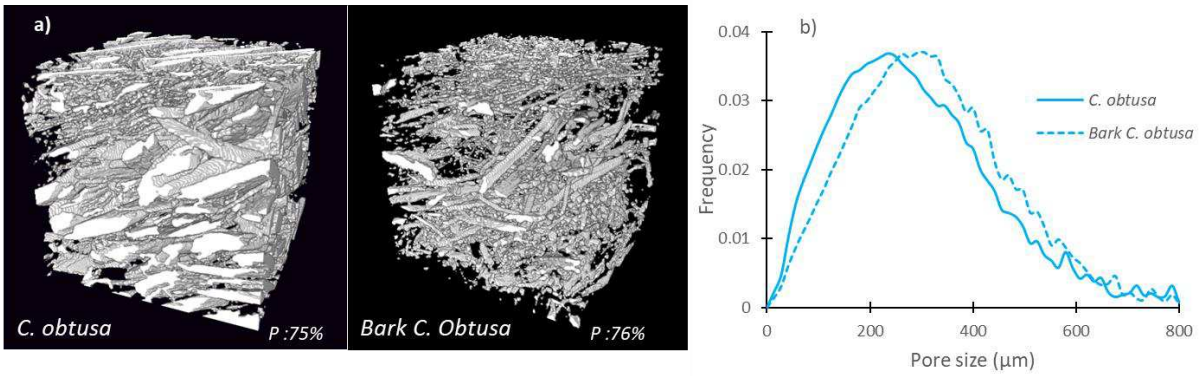

Figure 11. a) 3D volume elements reconstructed from successive X-ray projections, corresponding to the fiberboards made of *C. obtusa* (left) and *Bark C. obtusa* (right); *P*: porosity. b) Pore size distribution computed from the 3D volume elements.

Evaluation of fiberboards' performances

- *Insulation performances*

The thermal conductivity of the fiberboards produced in this study is illustrated in Figure 12, and compared to the commercial reference fiberboards made from pinewood (*Pinus pinaster*) (orange squares on Figure 12). For the commercial reference, testing samples of varying densities has shown that it exists an optimal density to achieve the lowest thermal conductivity (0.045 W.m^{-1}.K^{-1} for a fiberboard density of 60 kg.m^{-3} in this case) (Vignon, 2020). Because of the small size and low elongation of the fibers used in this work, compaction of the fiberboards was increased to obtain suitable cohesion of the mats. As a result, the density of the fiberboards produced in this study ranged between 141.9 and 267.7 kg.m^{-3}, hence corresponding to the upper range of the pinewood reference curve. Therefore, our results might not cover the optimum thermal conductivity / fiberboard density ratio reachable for each fraction. Nevertheless, without any optimization of the fiber morphological characteristics, the fiberboards produced in this study from tropical wood and bark have a thermal conductivity close to or even lower than those reported for the commercial reference considering the same density range (Figure 12). These results are promising and it is reasonable to assume that highly efficient insulating material could be produced from these resources with further optimization of fiber preparation and fiberboard manufacturing.

It is interesting to note that contrasting results were observed depending on the fibers used. *S. rubra and D. guianensis* wood-based fiberboards offer medium to high thermal conductivities, respectively, ranging from 0.04 W.m^{-1}.K^{-1} to 0.1 W.m^{-1}.K^{-1}. Quite high scattering of thermal conductivity values was noticed for these

samples, which might originate from the existing structural and chemical tree natural variability, already reported by several authors for these two species [32–34]. The natural variability of the fractions will be unavoidable, and must be considered in order to evaluate realistic final properties of the fiberboards produced from residual fibers. On the contrary, fiberboards produced from bark fractions showed the best and less scattered results, with equivalent to higher insulating performances compared to the commercial reference in the same density range. Belley (2009) suggested that mat density, fiber size and pore sizes mostly influence the thermal conductivity of fiber mats. Here, the small-sized bark particles could contribute to the creation of a specific pore network, thus promoting better insulation performance. Interestingly, for the *C. obtusa* species, a clear difference can be observed between fiberboards produced from wood or bark fractions. Indeed, despite easy processing and promising microstructuration, *C. obtusa* wood showed the poorest thermal performances, i.e., high thermal conductivity around 0.1 $W.m^{-1}.K^{-1}$.

Since no glue was used during the production of fiberboards (and given that synthetic fibers are not supposed to influence the material's thermal properties), and samples were stabilized to the same water content prior testing, thermal conductivity should only depend on the intrinsic properties of natural fibers used for the manufacturing of the boards, as well as the resulting microstructure of fiberboards, their overall porosity and pore size distribution [7, 36]. X-ray tomography confirmed that pore size distribution and porosity were similar for fiberboards made from wood and bark fibers of *C. obtusa*, with only slightly larger pores in bark-based fiberboards. This suggests that the good thermal conductivities obtained for fiberboards produced from bark fibers could be related to the good intrinsic thermal properties of the fibers. This assumption seems consistent with the fact that bark fibers naturally display protecting functions for the tree, including thermal insulation to resist to climate variations (T °C and RH). But further investigations are needed to better understand the insulating performance of bark-based fiberboards in relation to their microstructure.

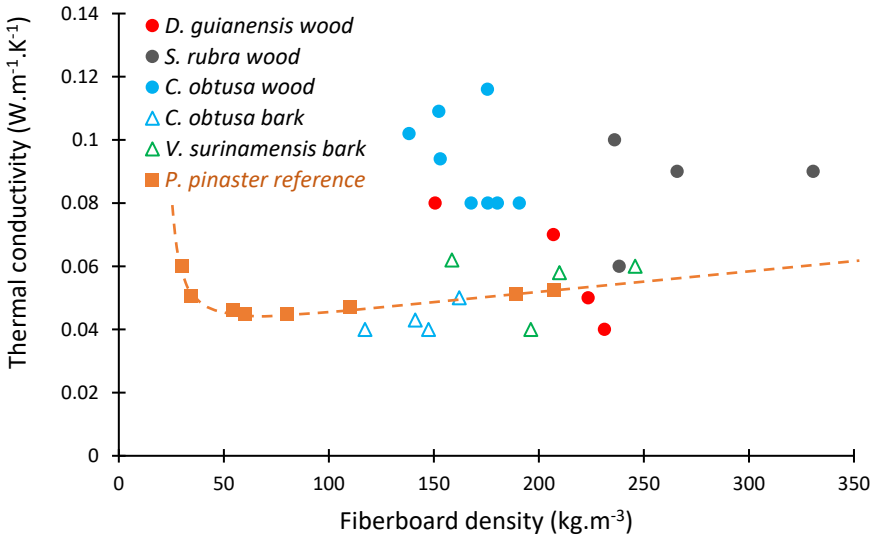

Figure 12. Evolution of the thermal conductivity of fiberboards as a function of their density at 12% of moisture content.

In summary, barks fibers from *C. obtusa* and *V. surinamensis* appear to be promising resources to produce insulation fiberboards, and wood fibers form *S. rubra* and *D. guianensis* show encouraging results. After improving the milling production step, to better control particle size and elongation and resulting fiberboards microstructure, even better insulating performance could be achieved. These results also raised an important point regarding the selection of the fractions. We observed that besides correct processing of the mats, the microporous network structure of the mat and the specific properties of the selected fibers are critical for insulating performance.

- *Water affinity*

Finally, since the produced fiberboards are intended to be used for the insulation of local habitations, in a humid environment, their sensitivity to water need to be investigated. In French Guiana, relative humidity (RH) is high (ranging from 58% to 73%). Also, for outdoor applications, this moisture range is relevant since degradation by wood-decaying fungi occurs at high humidity levels. Affinity to water at high RH and behavior over several RH cycles is thus a key parameter to rule on the fiberboards' quality as insulating material under tropical conditions.

Figure 13 displays the obtained sorption isotherms for each fiberboard sample, where the stabilized values of moisture content (MC) are represented along five different RH stages for wood (solid lines) and bark fibers (dotted lines). The obtained curves superimposed at low RH stages but clearly differentiated at higher RH. Fiberboards produced from wood fibers showed lower maximal water uptake compared to the pinewood reference (at 90% RH: MC = 11.84% for *S. rubra*, 13.02% for *D. guianensis,* 14.02% for *C. obtusa* and 18% for the pinewood reference). Fiberboards produced from Bark *C. obtusa* and Bark *V. surinamensis* showed the highest values of water uptake at 90% RH (MC = 18.70% and 15.15%, respectively). Samples made from Bark *C. obtusa* showed a behavior very close to that of the reference pinewood fiberboard: MC already increases significantly at low RH stages (being in average more than 30% higher compared to other samples at 50% RH). Like the commercial pinewood reference, Bark *C. obtusa* thus showed a marked affinity to water compared to other studied species, which might be due to a high content of hemicellulose or low content of extractives.

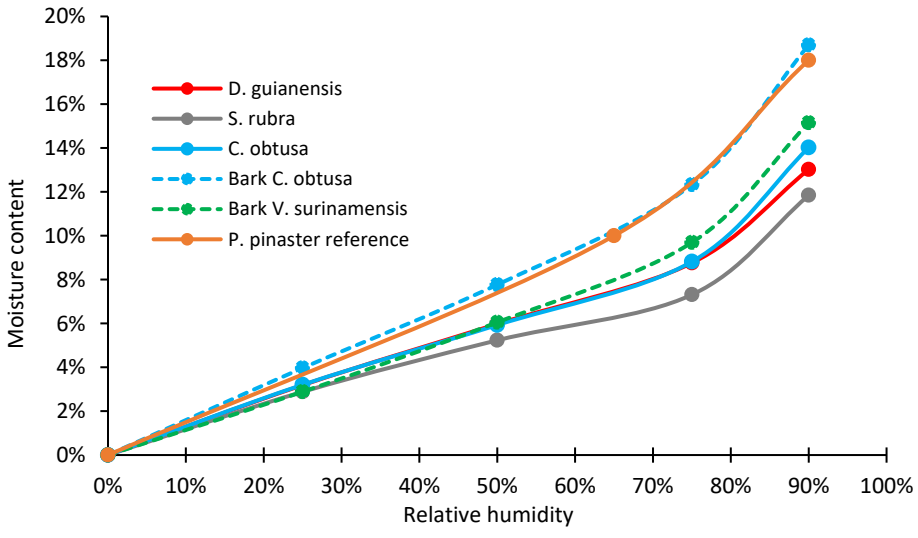

Figure 13. Sorption isotherms obtained for each fiberboard sample, using DVS. Wood species are presented in solid lines while bark species are represented in dotted lines. The influence of relative humidity on moisture content is represented at each RH stage. Stabilized moisture content values consist in the quantity of water sorbed by the samples after reaching the equilibrium criteria of dm/dt < 0.001%.

In addition to the stabilized values (MC), it is also interesting to study the kinetics of moisture sorption since great humidity fluctuations can be observed in French Guiana at day-scale between mid-day (59%RH at 11:00am) and night (92%RH at 05:00am). The specific mass stabilization time (*SMST*, corresponding to the time per unit of mass necessary to reach a mass equilibrium after a change in RH from 75% to 90%) is reported for each sample on Figure 14. For fiberboards made from wood fibers, variations in SMST seems to be related to variations in fiber density and extractive content (see Table 1). Indeed, sorption mechanisms could be influence by the hydrophilicity of extractives and fiber cell wall microporosity, making the sorption sites more or less accessible [37, 38].

Compared to wood fibers, bark fibers *(i)* absorb a larger amount of water at high RH (Figure 13) but *(ii)* need a longer time to reach saturation (highest values of SMST). Because of their strong affinity for water, bark fiberboards might fluctuate in the critical range of moisture content favorable for fungal degradation. It thus points out the need of investigating their durability in service-use conditions. However, to protect the tree against pests and diseases, bark generally contains more extractives than wood and is expected to be naturally durable. For example, Morris, Grace, and Troughton (1999) reported good natural durability for a board material made from pressed spruce bark with no additives. As evidenced for oak wood, the inhibiting effect of tannins and suberin on fungal growth could bring a higher resistance to the bark than to the wood [40]. Bark extracts are even considered for developing new bio-based preservative treatments to improve the biological resistance of wood [41]. Finally, fiberboards produced from bark fibers might also be of interest for humidity regulation: they might act as water buffers since water sorption kinetics is slower compared to wood.

These hypotheses must be verified through long-term and RH cycling experiments. A perspective of this work would be to conduct tests on the produced fiberboards in real service-use conditions to assess *(i)* their durability and *(ii)* their insulating performance under fluctuating humidity conditions.

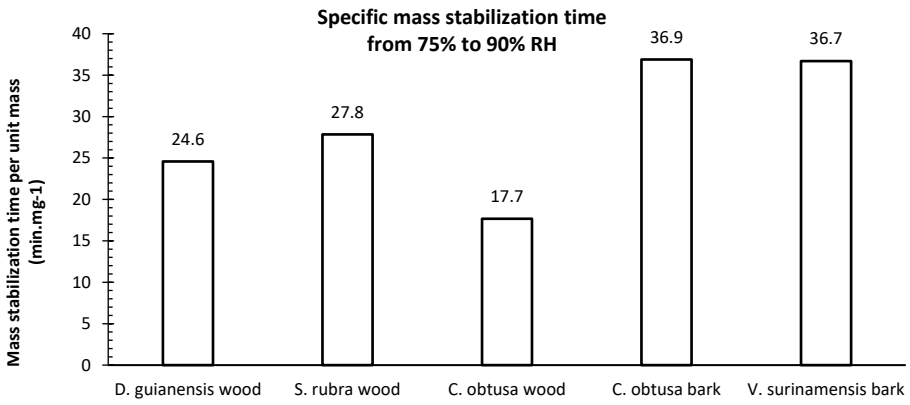

Figure 14. Average specific mass stabilization time (SMST), corresponding to the time per unit of mass necessary to reach mass equilibrium after RH variation from 75% to 90%.

CONCLUSION

This study was a first basis of prospection to evaluate the potential of Guyanese waste fibers for the production of insulation fiberboards. Wood residues from two of the most common local commercial species (*D. guianensis* and *S. rubra*) and from an abundant fast-growing species (*C. obtusa*), as well as bark fibers of interest (Bark *C. obtusa* and Bark *V. surinamensis*), were selected and harvested to manufacture bio-based insulation fiberboards. Fiberboards were produced from milled fiber fractions according to an environmentally friendly process using the self-bonding properties of the fibers and a small fraction of synthetic fibers.

The morphological analysis operated on the milled fractions highlighted the need for an optimization of the milling process to achieve suitable fiber/particle size and shape. Regarding fiberboards production, adjustments had to be made according to the specific morphology of the obtained fractions. Processing parameters were optimized to limit mass losses and favor mat cohesion. Our results showed that fibers shape is a key morphological parameter to be considered for fiberboards manufacturing process. It appeared to positively influence self-bonding of the fibers, improving fiberboards cohesion. However, in addition to the proper manufacturing of the fiber mats, the specific properties of the selected fibers are likely to influence the performances of the fiberboards at first order.

Regarding final thermal insulation performance, despite no optimization of the fractions' dimensions and fiberboard densities, the fiberboards made from tropical wood and bark residues displayed quite interesting low thermal conductivities. Some of the selected residual fiber resources even enabled the production of fiberboards with performances comparable to those reported for the commercial reference. Bark fractions of *C. obtusa* and *V. surinamensis* appeared to be really promising materials and wood fractions of *S. rubra* and *D. guianensis* gave encouraging results. Moreover, bark fibers displayed the best resistance to thermal degradation and fire reaction, two parameters of interest for building applications. On the other hand, bark fibers were also characterized by higher affinity to water compared to wood fibers, showing the highest water uptake at 90% RH. However, we also reported longer stabilization time to reach equilibrium for bark fiberboards, which might be of interest for humidity regulation.

To go further, a future work will consist in developing in-situ, long-term RH cycling methods to better characterize the insulation performance of fiberboards. Indeed, temperature, moisture content and their variation/cycling are important parameters affecting thermal properties of wood and wood-based materials. New quantitative data are required to assess thermal conductivity and durability of insulation fiberboards in real conditions of use. In conclusion, it was possible to produce competitive insulation fiberboards from tropical residues, paving the way for promising future research.

ACKNOWLEDGMENT

This research project has been financially supported by a PEPS CNRS-INSIS grant.

The authors are grateful to the French National Research Agency (ANR) for its financial support through the Xylomat project, Equipex XYLOFOREST (ANR-10-EQPX-16).

The authors thank Romain Lehnebach and Leopold Doumerc for providing bark material.

The authors thank the PLANET facility (doi: 10.15454/1.5572338990609338E12) run by the IATE joint research unit for its process experiment supports.

The authors thank Sophie Bezaud (student at Bordeaux Sciences Agronomique) and Doriane Beauseroy, Amanda Ribas Leão and Frédéric Pécot (students at the Ecole Supérieure du Bois engineering school) for their contributions to the experimental part.

References

REFERENCE LIST

1. Hobballah, M.H., Ndiaye, A., Michaud, F., Irle, M.: Formulating preliminary design optimization problems using expert knowledge: Application to wood-based insulating materials. Expert Syst. Appl. 92, 95–105 (2018). https://doi.org/10.1016/j.eswa.2017.09.035
2. Schiavoni, S., D'Alessandro, F., Bianchi, F., Asdrubali, F.: Insulation materials for the building sector: A review and comparative analysis, (2016)
3. Latif, E., Lawrence, R.M.H., Shea, A.D., Walker, P.: An experimental investigation into the comparative hygrothermal performance of wall panels incorporating wood fibre, mineral wool and hemp-lime. Energy Build. 165, 76–91 (2018). https://doi.org/10.1016/J.ENBUILD.2018.01.028
4. Porter, M., Yu, J.: Crystallization Kinetics of Poly(3-hydroxybutyrate) Granules in Different Environmental Conditions. J. Biomater. Nanobiotechnol. 02, 301–310 (2011). https://doi.org/10.4236/jbnb.2011.23037
5. Lehnebach, R., Alméras, T., Clair, B.: How does bark contribution to postural control change during tree ontogeny? A study of six Amazonian tree species. J. Exp. Bot. 71, 2641–2649 (2020). https://doi.org/10.1093/jxb/eraa070
6. Vignon, P., Hobballah, H.M., Moreau, J., Delisée, C., Irle, M.: Optimization of the thermal properties of wood fiber-based insulating materials. In: Hygrothermal performance of buildings and their materials, Joint Conference: COST Action FP1303 & DURAWOOD Project. , Poznan, Poland (2016)
7. Sonderegger, W.U.: Experimental and theoretical investigations on the heat and water transport in wood and wood-based materials. (2011). https://doi.org/10.3929/ethz-a-006532317
8. Vignon, P., Hobballah, M.H., Tran, H., Moreau, J., Delisée, C., Lecourt, M., Belalia, R., Sanguina, T.: Thermal insulating materials made up of poplar wood fibres. In: 2nd Conference on Engineered Wood Products based on Poplar/Willow Wood CEWPPW2. , Leon, Spain (2016)
9. Mayer-Laigle, C., Rajaonarivony, R., Blanc, N., Rouau, X.: Comminution of Dry Lignocellulosic Biomass: Part II. Technologies, Improvement of Milling Performances, and Security Issues. Bioengineering. 5, 50 (2018). https://doi.org/10.3390/bioengineering5030050
10. Hill, C.A.S., Norton, A.J., Newman, G.: The water vapour sorption properties of Sitka spruce determined using a dynamic vapour sorption apparatus. Wood Sci. Technol. 44, 497–514 (2010). https://doi.org/10.1007/s00226-010-0305-y
11. Engelund, E.T., Klamer, M., Venås, M.: Acquisition of sorption isotherms for modified woods by the use of dynamic vapour sorption instrumentation: principles and practice. 41st Annu. Meet. Int. Res. Gr. Wood Prot. Biarritz, Fr. 9-13 May 2010. (2010)
12. David, G.: Eco-conversion de résidus lignocellulosiques de l'agriculture en matériaux composites durables à matrice biopolyester., (2019)

13. Rajaonarivony, K., Rouau, X., Lampoh, K., Delenne, J.Y., Mayer-Laigle, C.: Fine comminution of pine bark: How does mechanical loading influence particles properties and milling efficiency? Bioengineering. 6, (2019). https://doi.org/10.3390/bioengineering6040102
14. Maharani, R., Yutaka, T., Yajima, T., Minoru, T.: Scrutiny on Physical Properties of Sawdust from Tropical Commercial Wood Species: Effects of Different Mills and Sawdust's Particle Size. Indones. J. For. Res. 7, 20–32 (2010). https://doi.org/10.20886/ijfr.2010.7.1.20-32
15. Vignon, P.: Caractérisation et Optimisation des propriétés d'isolants thermiques non tissés à base de fibres de bois, (2020)
16. Gil, M. V., Casal, D., Pevida, C., Pis, J.J., Rubiera, F.: Thermal behaviour and kinetics of coal/biomass blends during co-combustion. Bioresour. Technol. 101, 5601–5608 (2010). https://doi.org/10.1016/j.biortech.2010.02.008
17. Kong, B., Wang, E., Li, Z., Lu, W.E.I.: Study on the feature of electromagnetic radiation under coal oxidation and temperature rise based on multifractal theory. Fractals. 27, (2019). https://doi.org/10.1142/S0218348X19500385
18. Cai, P., Nie, W., Chen, D., Yang, S., Liu, Z.: Effect of air flowrate on pollutant dispersion pattern of coal dust particles at fully mechanized mining face based on numerical simulation. Fuel. 239, 623–635 (2019). https://doi.org/10.1016/j.fuel.2018.11.030
19. Cheng, K., Winter, W.T., Stipanovic, A.J.: A modulated-TGA approach to the kinetics of lignocellulosic biomass pyrolysis/combustion. Polym. Degrad. Stab. 97, 1606–1615 (2012). https://doi.org/10.1016/j.polymdegradstab.2012.06.027
20. Dorez, G., Ferry, L., Sonnier, R., Taguet, A., Lopez-Cuesta, J.M.: Effect of cellulose, hemicellulose and lignin contents on pyrolysis and combustion of natural fibers. J. Anal. Appl. Pyrolysis. 107, 323–331 (2014). https://doi.org/10.1016/j.jaap.2014.03.017
21. López-Beceiro, J., Díaz-Díaz, A.M., Álvarez-García, A., Tarrío-Saavedra, J., Naya, S., Artiaga, R.: The Complexity of Lignin Thermal Degradation in the Isothermal Context. Process. 2021, Vol. 9, Page 1154. 9, 1154 (2021). https://doi.org/10.3390/PR9071154
22. Di Blasi, C.: Combustion and gasification rates of lignocellulosic chars, (2009)
23. Burhenne, L., Messmer, J., Aicher, T., Laborie, M.P.: The effect of the biomass components lignin, cellulose and hemicellulose on TGA and fixed bed pyrolysis. J. Anal. Appl. Pyrolysis. 101, 177–184 (2013). https://doi.org/10.1016/J.JAAP.2013.01.012
24. Haurie, L., Giraldo, M.P., Lacasta, A.M., Montón, J., Sonnier, R.: Influence of different parameters in the fire behaviour of seven hardwood species. Fire Saf. J. 107, 193–201 (2019). https://doi.org/10.1016/j.firesaf.2018.08.002
25. Şen, A., Van den Bulcke, J., Defoirdt, N., Van Acker, J., Pereira, H.: Thermal behaviour of cork and cork components. Thermochim. Acta. 582, 94–100 (2014). https://doi.org/10.1016/j.tca.2014.03.007
26. Taipale, T., Österberg, M., Nykänen, A., Ruokolainen, J., Laine, J.: Effect of microfibrillated cellulose and fines on the drainage of kraft pulp suspension and paper strength. Cellulose. 17, 1005–1020 (2010). https://doi.org/10.1007/s10570-010-9431-9

27. Stark, N.M.: Effects of wood fiber characteristics on mechanical properties of wood / polypropylene composites. (2003)
28. Hashim, R., Nadhari, W.N.A.W., Sulaiman, O., Kawamura, F., Hiziroglu, S., Sato, M., Sugimoto, T., Seng, T.G., Tanaka, R.: Characterization of raw materials and manufactured binderless particleboard from oil palm biomass. Mater. Des. 32, 246–254 (2011). https://doi.org/10.1016/j.matdes.2010.05.059
29. Börcsök, Z., Pásztory, Z.: The role of lignin in wood working processes using elevated temperatures: an abbreviated literature survey. Eur. J. Wood Wood Prod. 2020 793. 79, 511–526 (2020). https://doi.org/10.1007/S00107-020-01637-3
30. Tran, H., Doumalin, P., Delisee, C., Dupre, J.C., Malvestio, J., Germaneau, A.: 3D mechanical analysis of low-density wood-based fiberboards by X-ray microcomputed tomography and Digital Volume Correlation. J. Mater. Sci. 48, 3198–3212 (2013). https://doi.org/10.1007/s10853-012-7100-0
31. Hamdi, S.E., Delisée, C., Malvestio, J., Beaugrand, J., Berzin, F.: Monitoring the Diameter Changes of Flax Fibre Elements during Twin Screw Extrusion Using X-Ray Computed Micro-Tomography. J. Nat. Fibers. 17, 1159–1170 (2020). https://doi.org/10.1080/15440478.2018.1558149
32. Lehnebach, R., Bossu, J., Va, S., Morel, H., Amusant, N., Nicolini, E., Beauchêne, J.: Wood Density Variations of Legume Trees in French Guiana along the Shade Tolerance Continuum: Heartwood Effects on Radial Patterns and Gradients. Forests. 10, 80 (2019). https://doi.org/10.3390/f10020080
33. Flora, C.: Origine et prédiction de la variabilité de la durabilité naturelle chez Dicorynia guianensis Amsh. Guyane (2018)
34. Houël, E., Rodrigues, A.M.S., Nicolini, E.-A., Ngwete, O., Duplais, C., Stien, D., Amusant, N.: Natural durability of Sextonia rubra, an Amazonian tree species: description and origin, (2017)
35. Belley, D.: Détermination des propriétés de transfert de chaleur et de masse des panneaux de fibres de bois. (2009)
36. Suleiman, B.M., Larfeldt, J., Leckner, B., Gustavsson, M.: Thermal conductivity and diffusivity of wood. Wood Sci. Technol. 33, 465–473 (1999). https://doi.org/10.1007/s002260050130
37. Wangaard, F.F., Granados, L.A.: The effect of extractives on water-vapor sorption by wood. Wood Sci. Technol. 1, 253–277 (1967). https://doi.org/10.1007/BF00349758
38. Choong, E.T., Achmadi, S.S.: Effect of extractives on moisture sorption and shrinkage in tropical woods. (1991)
39. Morris, P.L., Grace, J.K., Troughton, G.E.: Preliminary Indications of the Natural Durability of Spruce Bark Board . (1999)
40. Vane, C.H., Drage, T.C., Snape, C.E.: Bark decay by the white-rot fungus Lentinula edodes: Polysaccharide loss, lignin resistance and the unmasking of suberin. Int. Biodeterior. Biodegrad. 57, 14–23 (2006). https://doi.org/10.1016/j.ibiod.2005.10.004
41. Lajnef, L., Caceres, I., Trinsoutrot, P., Charrier-El Bouhtoury, F., Ayed, N., Charrier, B.: Effect of Punica granatum peel and Melia azedarach bark extracts on durability of European beech and maritime pine. Eur. J. Wood Wood Prod. 76, 1725–1735 (2018). https://doi.org/10.1007/s00107-018-1340-x

Statements & Declarations

FUNDING

This research project has been financially supported by a PEPS CNRS-INSIS grant.

The authors are grateful to the French National Research Agency (ANR) for its financial support through the Xylomat project, Equipex XYLOFOREST (ANR-10-EQPX-16).

COMPETING INTERESTS

The authors have no relevant financial or non-financial interests to disclose.

AUTHOR CONTRIBUTIONS

J. Bossu contributed to the study conception and design. Material preparation, data collection and analysis were performed by J. Bossu, J. Moreau, C. Delisee and R. Sonnier. The first draft of the manuscript was written by J. Bossu and all authors commented on previous versions of the manuscript. All authors read and approved the final manuscript.

DATA AVAILABILITY

The datasets generated during and/or analyzed during the current study are available in the “Guyavalofibres” repository, https://doi.org/10.18167/DVN1/KVNAQ6.